Hydrodynamical modes and light scattering in the liquid-crystalline cubic blue phases. II. Dynamic theory

Holger Stark*
Department of Physics, University of Pennsylvania, Philadelphia, Pennsylvania 19104

Hans-Rainer Trebin
Institut für Theoretische und Angewandte Physik, Universität Stuttgart, Pfaffenwaldring 57, 70550 Stuttgart, Germany
(Received 23 August 1994)

As shown in the preceding paper, the hydrodynamical modes of the cubic blue phases are displacement modes, which are equivalent to acoustic phonons in crystal. We apply the model of a viscoelastic mixture to describe their dynamics. For the transverse modes the dispersion relations do not show the expected power-law behavior of the hydrodynamical regime. Instead they display a flat, widely extended minimum that explains the strange dynamics of light-scattering experiments in cubic blue phases. Within the kinematical theory of light scattering we propose special geometries for measuring the material parameters of the viscoelastic mixture. To understand the forescattering, commonly observed in experiments, and the strong dependence of the fluctuating light intensity on the incident wavelength, we extend our calculation to the more general dynamical theory. A qualitative interpretation of the experiments suggests that the cubic blue phases are highly anisotropic with regard to their viscous behavior.

PACS number(s): 61.30.−v, 47.35.+i, 42.25.Fx

I. INTRODUCTION

In the preceding paper [1] we studied the elastic theory for the orientational pattern of the cubic blue phases (BPs) I and II. For the long-wavelength limit we were able to identify the hydrodynamical modes with displacement modes and we found that the elastic tensor of the displacement modes had to be renormalized due to coupling to other deformation modes.

This article is devoted to the dynamical behavior of the displacement modes, which are completely described by the displacement field $\boldsymbol{u}(\boldsymbol{r})$ as the hydrodynamical variable. In Sec. II B we are going to formulate the hydrodynamical equations and investigate the eigenmodes. Their dispersion relations can be measured in light scattering experiments with special geometries. We will propose several geometries within the kinematical theory in Sec. III A.

Marcus [2] was the first to observe strong fluctuations in the intensity of light reflected from the orientational pattern of the molecules, close to Bragg reflections. He used a backscattering geometry where the wave vectors $\boldsymbol{k}_i$ and $\boldsymbol{k}_f$ of the incident and scattered light were almost antiparallel. He argued that the same fluctuations also had to be seen in forescattering. Hence further investigations [3] were performed in forescattering with scattering vectors $\boldsymbol{q}_s = \boldsymbol{k}_f - \boldsymbol{k}_i$ ranging from $q_s/k = 0.001$ to 0.04, compared to the reciprocal lattice vector $\boldsymbol{k} = (100)$ of the Bragg reflection. Analyzing the time correlation function $\langle E_s^*(0)\, E_s(t)\rangle$ of the scattered electric field, Marcus obtained a superposition of two exponential functions

$$\langle E_s(0)\, E_s(t)\rangle \propto \exp[-z_1(q_s)t] + 0.62\, \exp[-z_2(q_s)t], \qquad t > 0 \tag{1}$$

with relaxation frequencies

$$z_1(q_s) = 785\ \mathrm{s}^{-1}, \qquad z_2(q_s) = 2262\ \mathrm{s}^{-1}\ . \tag{2}$$

Surprisingly, the frequencies did not depend on q_s and remained finite for $q_s \to 0$. This is an unusual behavior for hydrodynamical modes, which we aim to explain in this article. Domberger [4] used larger scattering vectors ranging from $q_s/k = 0.14$ to 0.28. He also found two relaxation frequencies, but only one dispersion relation showed a definitely finite value, 400 s^{-1}, for $q_s \to 0$. The other dispersion relation tends towards a finite value of 100 s^{-1} for the relaxation frequency at $q_s = 0$, but, as the experiment could not get too close to vanishing wave vectors, this is not completely certain. Both authors realized strong coupling between the fluctuating light and the Bragg reflected light. When the incident wavelength was chosen on the edges of the Bragg band the fluctuations were about 6% of the peak intensity. They considerably decreased in the center or outside the Bragg band. This behavior cannot be understood within the kinematical theory. Therefore we have extended the calculations to the more general dynamical theory (see Sec. III B). It determines the electromagnetic field in the scattering

*Permanent address: Institut für Theoretische und Angewandte Physik, Universität Stuttgart, Pfaffenwaldring 57, 70550 Stuttgart, Germany.

material in a self-consistent way. Also the forescattering experiments can only be explained within the dynamical theory, as we will show in Sec. III A.

II. HYDRODYNAMICAL BEHAVIOR OF THE DISPLACEMENT MODES

A. Overview

In the preceding paper [1] we extracted the displacement modes from the Landau–de Gennes free energy, expanded in the order parameter field $\boldsymbol{\mu}(\boldsymbol{r})$, and calculated the elastic constants depending on the Landau coefficients and the amplitudes $\mu_2(\boldsymbol{k})$ of the helical tensor modes. In the same manner we could derive the dynamical equations of the displacement field and its viscosities. To describe the alignment of the molecules in the cubic blue phases we choose the local inertia tensor density $\boldsymbol{\Theta}(\boldsymbol{r})$ of a small volume as an order parameter. It appears in the balance equation of the angular momentum. The problem is that in the blue phases, the principal axes of $\boldsymbol{\Theta}(\boldsymbol{r})$ and the principal moments of inertia change from point to point. Hence we have to consider the blue phases locally as a nonrigid body, known in the literature as a *Cosserat* continuum [5]. Its dynamical equations are not yet fully established [5,6]. Only in the special case of the nematic phase, where the inertia tensor is rigid and uniaxial, can the Leslie-Ericksen equations be deduced from the balance equations of momentum and angular momentum [7]. To formulate the dynamical equations of the displacement field we need another method.

B. Hydrodynamical equations

We view a cubic blue phase as a *viscoelastic mixture*. The first component, the viscous fluid, describes the motion of the centers of mass of the molecules by the mass density $\varrho(\boldsymbol{r},t)$ and the velocity field $\boldsymbol{v}(\boldsymbol{r},t)$. The second component stands for the orientational pattern. Its elastic deformation is characterized by a displacement field $\boldsymbol{u}(\boldsymbol{r},t)$ of the periodic lattice. The motion of each component obeys a balance equation of momentum. Both equations are coupled by a force fulfilling Newton's third law *action = reaction*. Balance equations for mass and energy are also taken into account. Then the application of the theory of mixtures [8,9] leads to a full set of hydrodynamical equations including temperature, whose derivation will be published elsewhere [10,11]. We are only interested in low-frequency modes. A careful analysis of the equations including estimates of the material parameters justifies the neglect of temperature and mass density variations: $\delta T = 0$ and $\delta\varrho = 0$ [10,11]. The second relation is the condition for an incompressible fluid. After linearization the resulting equations are

$$\mathbf{0} = -k_P\left(\frac{\partial \boldsymbol{u}}{\partial t} - \boldsymbol{v}\right) + \boldsymbol{\lambda}(\nabla\otimes\nabla)\boldsymbol{u}, \tag{3}$$

$$\varrho\frac{\partial \boldsymbol{v}}{\partial t} = k_P\left(\frac{\partial \boldsymbol{u}}{\partial t} - \boldsymbol{v}\right) + [\boldsymbol{\eta}(\nabla\otimes\nabla)]_t\boldsymbol{v}\ ,\ \ \mathrm{div}\boldsymbol{v} = 0, \tag{4}$$

with

$$\boldsymbol{\lambda}(\nabla\otimes\nabla) = \lambda\Delta + (\lambda+\lambda')\mathrm{grad}\,\mathrm{div} + \lambda_K\sum_{i=1}^{3}(\boldsymbol{P}_i\nabla)^2\boldsymbol{P}_i, \tag{5}$$

$$[\boldsymbol{\eta}(\nabla\otimes\nabla)]_t = \eta\Delta + \eta_K\sum_{i=1}^{3}(\boldsymbol{P}_i\nabla)^2\boldsymbol{P}_i\ . \tag{6}$$

Apart from the first term on the right-hand side, Eq. (3) is the dynamical relation of the linear elasticity theory of solids where inertial effects of the orientational pattern are neglected [10,11]. The shorthand notation $\boldsymbol{\lambda}(\nabla\otimes\nabla)$ [see Eq. (5)] is defined just as in [1] if the wave vector $\boldsymbol{q}$ is replaced by the Nabla operator ∇. Equations (4) are the Navier-Stokes equations for an incompressible fluid. The operator $\boldsymbol{\eta}(\nabla\otimes\nabla)$ is to be interpreted as $\boldsymbol{\lambda}(\nabla\otimes\nabla)$. In particular, we have to introduce a viscosity η_K which takes into account the cubic point symmetry of the fluid. The index t stands for the restriction to velocity fields $\boldsymbol{v}(\boldsymbol{r})$ with a vanishing divergence and hence having transverse components only. The equations are coupled by the *permeation term*, a friction force proportional to the relative velocity of the viscous fluid and the orientational pattern. The *permeation coefficient* k_P is an Onsager coefficient like η and η_K [10,11]. The microscopic origin of the permeation is the following: As molecules flow through the stationary orientational pattern, their axes must follow the local order parameter. However, their reorientation is hindered by collisions between the molecules, which lead to a rotational viscosity. The permeation was first introduced by Helfrich for the cholesteric helix [12]. Following his calculations we estimate the permeation coefficient as

$$k_P = \gamma_1\left(\frac{2\pi}{b}\right)^2 \approx 10^{10}\,\frac{\mathrm{g}}{\mathrm{cm^3\,s}}\ , \tag{7}$$

where γ_1 is the rotational viscosity appearing in the Leslie-Erickson equations [13]. We assume a value of 0.1 P for γ_1 and for the lattice constant b of 2×10^{-5} cm. The elastic constants were calculated in [1]:

$$\lambda \approx 1000\,\frac{\mathrm{ergs}}{\mathrm{cm^3}}\ ,\ \ \lambda'/\lambda \approx 0.6,\quad \lambda_K/\lambda \approx \pm 0.3\ . \tag{8}$$

For the viscosity η we take a standard value [13] $\eta = 1$ P, while for η_K there is no estimate. The mass density ϱ is approximately 1 g/cm^3 [14]. The scaled reciprocal permeation coefficient

$$\tau_P = \frac{\varrho\lambda}{\eta}\,\frac{1}{k_P} \approx 10^{-7} \ll 1 \tag{9}$$

is an important quantity of our system. Because of its small value, the friction force between the two components is very large and the molecules can hardly flow through a stationary orientational pattern, as has been

measured by Stegemeyer and Pollmann [15]. This feature influences the dynamical behavior of the blue phases and is the reason why we can neglect temperature variations [10,11]. Equations (3) and (4) also appear in the dynamical equations of colloidal crystals [16–20]. They have been used already to analyze mechanical experiments in blue phases [21–23].

For the solution of the dynamical equations we introduce a plane wave ansatz

$$\boldsymbol{d}(\boldsymbol{r},t) := \begin{pmatrix} u_l(\boldsymbol{r},t) \\ \boldsymbol{u}_t(\boldsymbol{r},t) \\ \boldsymbol{v}_t(\boldsymbol{r},t) \end{pmatrix} = \begin{pmatrix} u_l(\boldsymbol{q}) \\ \boldsymbol{u}_t(\boldsymbol{q}) \\ \boldsymbol{v}_t(\boldsymbol{q}) \end{pmatrix} \exp(-zt + i\boldsymbol{q}\cdot\boldsymbol{r}) \ . \tag{10}$$

The displacement field is divided into its longitudinal (index l) and transverse (index t) components. $\boldsymbol{v}$ only contains a transverse component as a conseqence of $\mathrm{div}\boldsymbol{v} = 0$.

From Eqs. (3) and (4) we obtain the generalized eigenvalue problem

$$\begin{pmatrix} -\boldsymbol{\lambda}(\boldsymbol{q}\otimes\boldsymbol{q}) + zk_P\,\mathbf{1} & \mathbf{0} \\ \mathbf{0} \quad -zk_P\,\mathbf{1}_t & k_P\,\mathbf{1}_t \\ & -[\boldsymbol{\eta}(\boldsymbol{q}\otimes\boldsymbol{q})]_t - k_P\,\mathbf{1}_t + z\mathbf{1}_t \end{pmatrix} \times \begin{pmatrix} u_l(\boldsymbol{q}) \\ \boldsymbol{u}_t(\boldsymbol{q}) \\ \boldsymbol{v}_t(\boldsymbol{q}) \end{pmatrix} = \mathbf{0} \tag{11}$$

or, in shorthand notation

$$\boldsymbol{D}(\boldsymbol{q},z)\,\boldsymbol{d}(\boldsymbol{q}) = \mathbf{0} \ . \tag{12}$$

The *dynamical matrix* $\boldsymbol{D}(\boldsymbol{q},\boldsymbol{z})$ appears as a block matrix. $\mathbf{1}_t$ means the identity tensor restricted to the plane perpendicular to $\boldsymbol{q}$. The nondiagonal elements have to be split because u_l does not couple directly to $\boldsymbol{v}_t$. The secular equation for $\boldsymbol{D}(\boldsymbol{q},\boldsymbol{z})$ leads to five dispersion relations $z(\boldsymbol{q})$. In general they cannot be expressed analytically. Therefore we will restrict ourselves to special directions of $\boldsymbol{q}$ in the next subsection.

C. Discussion of longitudinal and transverse modes

In [1] we analyzed the eigenvalue problem

$$\boldsymbol{\lambda}(\boldsymbol{q}\otimes\boldsymbol{q})\,\boldsymbol{u}(\boldsymbol{q}) = \lambda_{\mathrm{eff}} q^2\,\boldsymbol{u}(\boldsymbol{q}) \ . \tag{13}$$

For wave vectors $\boldsymbol{q}$ with a nontrivial little group $\mathcal{K}(\boldsymbol{q})$, we found longitudinal and transverse eigenmodes. The structure of the tensor $[\boldsymbol{\eta}(\boldsymbol{q}\otimes\boldsymbol{q})]_t$, the transverse part of $\boldsymbol{\eta}(\boldsymbol{q}\otimes\boldsymbol{q})$, is the same as the transverse part of $\boldsymbol{\lambda}(\boldsymbol{q}\otimes\boldsymbol{q})$ [compare Eqs. (5) and (6)]. Hence $[\boldsymbol{\eta}(\boldsymbol{q}\otimes\boldsymbol{q})]_t$ and $\boldsymbol{\lambda}(\boldsymbol{q}\otimes\boldsymbol{q})$ have the same transverse eigenvectors. Because the remaining tensors in $\boldsymbol{D}(\boldsymbol{q},z)$ are isotropic, the generalized eigenvalue problem (11) splits into the eigenvalue problem of the longitudinal mode

$$(-\lambda_{\mathrm{eff}} q^2 + zk_P)u_l(\boldsymbol{q}) = 0 \tag{14}$$

and two identical of transverse modes

$$\begin{pmatrix} -\lambda_{\mathrm{eff}} q^2 + zk_P & k_P \\ -zk_P & -\eta_{\mathrm{eff}} q^2 - k_P + z \end{pmatrix} \times \begin{pmatrix} u_t(\boldsymbol{q},z) \\ v_t(\boldsymbol{q},z) \end{pmatrix} = \mathbf{0} \ . \tag{15}$$

For the transverse case, λ_{eff} and the effective viscosity η_{eff} show the same dependence on λ, λ_K and η, η_K, respectively [1]. If the symmetry of $\mathcal{K}(\boldsymbol{q})$ is just a mirror plane, only one eigenvalue problem for a transverse mode can be separated from the general one of Eq. (11).

The dispersion relation

$$z_l(q) = \frac{\lambda_{\mathrm{eff}}}{k_P}\,q^2 \tag{16}$$

of a purely diffusive, longitudinal mode follows immediately from Eq. (14). The deformed orientational pattern relaxes slowly towards its equilibrium structure by moving through a fluid at rest which does not allow a longitudinal component of the velocity field. $z_l(q)$ is proportional to q^2, a behavior often found for hydrodynamical modes.

From Eq. (15) we obtain the dispersion relations of two transverse modes

$$z_{t1/2}(q) = \frac{1}{2}q^2\left(\frac{\eta_{\mathrm{eff}}}{\varrho} + \frac{\lambda_{\mathrm{eff}}}{k_P}\right) \pm iq\sqrt{\frac{\lambda_{\mathrm{eff}}}{\varrho}}\sqrt{1-\left(\frac{q}{q_b}\right)^2}, \tag{17}$$

where we have introduced the wave number

$$q_b = 2\,\frac{\sqrt{\lambda_{\mathrm{eff}}/\varrho}}{|\eta_{\mathrm{eff}}/\varrho - \lambda_{\mathrm{eff}}/k_P|} \ . \tag{18}$$

From the values of k_P, λ, η, and ϱ given in Sec. II B and with Eq. (9) we estimate

$$q_b \approx 2\,\frac{\sqrt{\varrho\lambda_{\mathrm{eff}}}}{\eta_{\mathrm{eff}}} \approx 63\ \mathrm{cm}^{-1} \tag{19}$$

or, relative to the lattice constant of the reciprocal lattice, $bq_b/2\pi \approx 2\times10^{-4}$. q_b gives rise to a bifurcation in the dispersion relation. We therefore discuss two ranges of q.

1. $q < q_b$. The elastic deformation of the orientational pattern allows two propagating modes. From Eq. (15) and condition (9) one finds for the velocity amplitudes

$$v_t(\boldsymbol{q},z) \approx -z_{t1/2}\,u_t(\boldsymbol{q},z) \ . \tag{20}$$

Because of the strong friction force, due to the permeation, the orientational pattern drags the fluid along when it relaxes towards its equilibrium structure. The relaxation frequency $\mathrm{Re}z_{t1/2}$ is determined by the viscosity of the fluid only. The oscillation frequency $\mathrm{Im}z_{t1/2}$ is shown in Fig. 1. Here and in the following figures the frequency and the wave number are given relative to

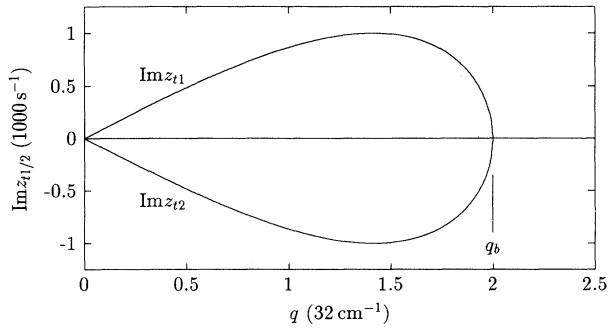

FIG. 1. Oscillation frequencies $\mathrm{Im}z_{t1/2}$ of the propagating transverse modes ($\boldsymbol{q}\|c_4$).

$$\frac{\lambda}{\eta} \approx 1000\ \frac{1}{\mathrm{s}}, \qquad \frac{\sqrt{\varrho\lambda}}{\eta} \approx 32\ \frac{1}{\mathrm{cm}}\ . \tag{21}$$

For small wave numbers $\mathrm{Im}z_{t1/2}$ is linear in q. The effective elastic constant λ_{eff} determines the phase velocity. For increasing wave numbers the oscillation frequency traverses an extremum at $q_b/\sqrt{2}$ and approaches zero at q_b with a vertical tangent.

The discussed range has been used in the above mentioned mechanical experiments of the blue phases [21–23]. The following range is important for light-scattering experiments.

2. $q > q_b$. Figure 2 contains a logarithmic plot of the relaxation frequency versus q^2. The wave vector is chosen parallel to a fourfold axis c_4. The largest value of q is approximately 10% of $2\pi/b$. The vanishing of the propagating modes is visible in a bifurcation of $\mathrm{Re}z_{t1/2}$ at q_b. Two branches grow out from one with a vertical tangent. The relaxation frequency at q_b is

$$z_{t1/2}(q_b) = 2\,\frac{\lambda_{\mathrm{eff}}}{\eta_{\mathrm{eff}}} \approx 2000\ \frac{1}{\mathrm{s}}. \tag{22}$$

In the case of $q \gg q_b$ we pull $-(q/q_b)^2$ out of the square root in Eq. (17) and expand it to the first order in q_b/q. This leads to the following approximations:

$$z_{t1}(q) = \frac{\eta_{\mathrm{eff}}}{\varrho}\,q^2 - \frac{\lambda_{\mathrm{eff}}}{\eta_{\mathrm{eff}}} \approx \frac{\eta_{\mathrm{eff}}}{\varrho}\,q^2 \tag{23}$$

$$z_{t2}(q) = \frac{\lambda_{\mathrm{eff}}}{k_P}\,q^2 + \frac{\lambda_{\mathrm{eff}}}{\eta_{\mathrm{eff}}}\ . \tag{24}$$

The two modes relax on different time scales as is clearly seen in Fig. 2. $z_{t1}(q)$ belongs to the damped transverse mode of a liquid. For light scattering we are only interested in the second, slowly relaxing mode. It shows a very unusual behavior. $\mathrm{Re}z_{t2}(q)$ goes through a flat, widely extended minimum and then increases slowly, proportional to q^2 with a slope typical for a longitudinal mode. The mimimum can be calculated via a Laurent expansion in $(\tau_P)^{1/4}$:

$$q_m \approx \left[\varrho k_P\,\frac{\lambda_{\mathrm{eff}}}{\eta_{\mathrm{eff}}^3}\right]^{1/4} \approx 1780\ \frac{1}{\mathrm{cm}} \approx 0.006\,\frac{2\pi}{b} \tag{25}$$

and

$$z_{t2}(q_m) \approx \frac{\lambda_{\mathrm{eff}}}{\eta_{\mathrm{eff}}} \approx 1000\ \frac{1}{\mathrm{s}}\ . \tag{26}$$

q_m is situated in the range of scattering vectors $\boldsymbol{q}_s$ used by Marcus [3] and, as we will show in Sec. III, his measured frequencies must be identified with $z_{t2}(q_m)$.

Figure 3 shows the relaxation frequencies of all three slowly relaxing modes with $\boldsymbol{q}\|c_2$ plotted versus q^2. Apart from the material parameters given in Sec. II B, we have chosen $\lambda_K/\lambda = 0.3$ and $\eta_K = 0$. The minimum is now situated close to $q^2 = 0$, and on this scale it appears as if the relaxation frequencies are finite for $q \to 0$. The values of $z_{t2}^{(1)}(q_m)$ and $z_{t2}^{(2)}(q_m)$ differ slightly due to $\lambda_K \neq 0$. As for $q < q_b$, we essentially find that the fluid and the orientational pattern approximately move with the same velocity. Nevertheless, for increasing q the fluid cannot completely follow the orientational pattern. For example, for $qb/2\pi \approx 0.1$ (that corresponds to the highest q value in Figs. 2 and 3) the velocities differ by 10%.

In the case of a general direction of the wave vector $\boldsymbol{q}$ we cannot decouple the eigenvalue problem of Eq. (11). One can show that the five dispersion relations do not admit common points and therefore are deformed com-

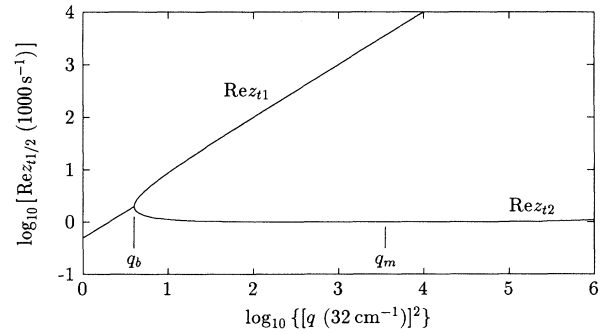

FIG. 2. Relaxation frequencies $\mathrm{Re}z_{t1/2}$ of the propagating transverse modes ($\boldsymbol{q}\|c_4$).

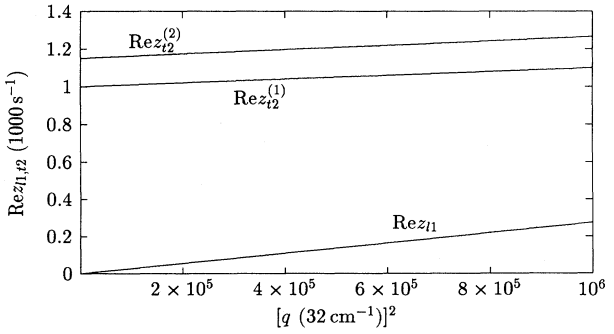

FIG. 3. Relaxation frequencies $\mathrm{Re}z_{l/t2}$ of the slowly relaxing transverse and longitudinal modes ($\boldsymbol{q}\|c_2$).

pared to the symmetry directions of $\boldsymbol{q}$. But, in principle, the five modes possess the same behavior. In particular, two of the three slowly relaxing modes will have the flat, widely extended minimum in their dispersion relations whereas the third will resemble the longitudinal mode.

D. Correlation functions

The discussion of light scattering in terms of displacement modes requires the time correlation function for the Fourier coefficients of the displacement field

$$\langle \boldsymbol{u}^*(\boldsymbol{q},t=0)\otimes\boldsymbol{u}(\boldsymbol{q},t)\rangle \ . \tag{27}$$

It will be determined by solving an initial-value problem. We assume a nonvanishing amplitude $\boldsymbol{u}(\boldsymbol{q},t=0)$ due to thermal excitations and want to know how it develops in time. We therefore introduce a Laplace and Fourier transformation of the dynamical equations (3) and (4). With the Fourier-Laplace transform

$$\boldsymbol{u}(\boldsymbol{q},z)=\int_0^\infty\int \boldsymbol{u}(\boldsymbol{r},t)\,\exp(zt-i\boldsymbol{q}\cdot\boldsymbol{r})\,d^3r\,dt \ , \tag{28}$$

and the same definition for $\boldsymbol{v}_t(\boldsymbol{q},z)$, we obtain

$$\boldsymbol{D}(\boldsymbol{q},z)\boldsymbol{d}(\boldsymbol{q},z)=\boldsymbol{A}\boldsymbol{d}(\boldsymbol{q},t=0), \tag{29}$$

where we have introduced a block matrix

$$\boldsymbol{A}=\begin{pmatrix} k_P\mathbf{1} & \mathbf{0} \\ \mathbf{0} & -k_P\mathbf{1}_t \quad \mathbf{1}_t \end{pmatrix} \ . \tag{30}$$

From Eq. (29) it follows that

$$\boldsymbol{d}(\boldsymbol{q},z)=\frac{1}{\det[\boldsymbol{D}(\boldsymbol{q},z)]}\,\widetilde{\boldsymbol{A}}(\boldsymbol{q},z)\,\boldsymbol{d}(\boldsymbol{q},t=0) \ . \tag{31}$$

The determinant

$$\det[\boldsymbol{D}(\boldsymbol{q},z)]=k_P^3\prod_{i=1}^{5}[z-z^{(i)}] \tag{32}$$

comes from $\boldsymbol{D}^{-1}(\boldsymbol{q},z)$ and $\widetilde{\boldsymbol{A}}(\boldsymbol{q},z)=\det[\boldsymbol{D}(\boldsymbol{q},z)]\,\boldsymbol{D}^{-1}(\boldsymbol{q},z)\boldsymbol{A}$. The transformation to the time variable yields [24]

$$\boldsymbol{d}(\boldsymbol{q},t)=\sum_{i=1}^{5}\lim_{z\to z^{(i)}}\frac{\widetilde{\boldsymbol{A}}(\boldsymbol{q},z^{(i)})\,[z-z^{(i)}]}{\det[\boldsymbol{D}(\boldsymbol{q},z)]}\times\exp[-z^{(i)}t]\,\boldsymbol{d}(\boldsymbol{q},t=0) \ , \ t\geq 0 \ . \tag{33}$$

The time correlation function (27) follows from Eq. (33) by an ensemble average. It involves the correlation function $\langle \boldsymbol{u}^*(\boldsymbol{q},t=0)\otimes\boldsymbol{v}(\boldsymbol{q},t=0)\rangle$, which vanishes because of its behavior under time reversal [25], and the mean square amplitude of the displacement field [26,27]

$$\langle \boldsymbol{u}^*(\boldsymbol{q})\otimes\boldsymbol{u}(\boldsymbol{q}')\rangle=\frac{k_BT}{V}\,\boldsymbol{\lambda}^{-1}(\boldsymbol{q}\otimes\boldsymbol{q})\,\delta_{\boldsymbol{q},\boldsymbol{q}'} \ . \tag{34}$$

V denotes the volume of the system. Equation (34) is understandable within the equipartition theorem. Note that there do not exist any correlations between different amplitudes in the system of eigenvectors because $\boldsymbol{\lambda}^{-1}(\boldsymbol{q}\otimes\boldsymbol{q})$ then has diagonal form. A general determination of the time correlation function is not possible since the zeros $z^{(i)}$ are not known. Thus we restrict ourselves to symmetry directions of $\boldsymbol{q}$.

1. *Longitudinal modes.* The amplitude $u_l(\boldsymbol{q},z)$ does not couple to the velocity field. We get

$$u_l(\boldsymbol{q},z)=\frac{u_l(\boldsymbol{q},t=0)}{-\lambda_{\rm eff}q^2/k_P+z}, \tag{35}$$

and after the transformation to the time variable the only nonvanishing time correlation function is

$$\langle u_l^*(\,q,t=0)\,u_l(\,q,t)\rangle=\frac{k_BT}{V}\,\frac{1}{\lambda_{\rm eff}q^2}\,\exp(-z_lt). \tag{36}$$

2. *Transverse modes.* The time evolution of $u_t(\boldsymbol{q},t)$ and $v_t(\boldsymbol{q},t)$ for $q\gg q_b$ reads

$$\begin{pmatrix} u_t(\boldsymbol{q},t) \\ v_t(\boldsymbol{q},t)\end{pmatrix}\approx\left[\begin{pmatrix} -\dfrac{\lambda_{\rm eff}}{(\eta_{\rm eff}q)^2} & -\dfrac{1}{\eta_{\rm eff}q^2} \\ \dfrac{\lambda_{\rm eff}}{\eta_{\rm eff}} & 1\end{pmatrix}\exp(-z_{t1}t) + \begin{pmatrix} 1 & \dfrac{1}{\eta_{\rm eff}q^2} \\ -\dfrac{\lambda_{\rm eff}}{\eta_{\rm eff}} & -\dfrac{\lambda_{\rm eff}}{(\eta_{\rm eff}q)^2}\end{pmatrix}\exp(-z_{t2}t)\right]\times\begin{pmatrix} u_t(\boldsymbol{q},t=0) \\ v_t(\boldsymbol{q},t=0)\end{pmatrix}. \tag{37}$$

We neglect the small, fast relaxing contribution from z_{t1} and get

$$\langle u_t^*(\boldsymbol{q},t=0)u_t(\boldsymbol{q},t)\rangle\approx\frac{k_BT}{V}\,\frac{1}{\lambda_{\rm eff}q^2}\,\exp(-z_{t2}t). \tag{38}$$

In fact, the thermally excited displacement modes also couple to microscopic excitations of the system. In the dynamical equations this coupling has to be taken into account by a stochastic force. But the ensemble average of this stochastic force vanishes [25] and our calculations of the correlation functions are correct. Hence the complete information about the displacement modes is contained in $\langle \boldsymbol{u}^*(\boldsymbol{q},t=0)\otimes\boldsymbol{u}(\boldsymbol{q},t)\rangle$.

III. LIGHT SCATTERING FROM DISPLACEMENT MODES

Light scattering is governed by the inhomogeneous part $\delta\boldsymbol{\varepsilon}(\boldsymbol{r},t)$ of the dielectric tensor $\boldsymbol{\varepsilon}(\boldsymbol{r},t)=\bar{\boldsymbol{\varepsilon}}+\delta\boldsymbol{\varepsilon}(\boldsymbol{r},t)$. In cubic blue phases the average $\bar{\boldsymbol{\varepsilon}}$ is isotropic

$$\bar{\boldsymbol{\varepsilon}}=\bar{\varepsilon}\mathbf{1}=\frac{1}{3}\,\mathrm{tr}\boldsymbol{\varepsilon}(\boldsymbol{r},t) \tag{39}$$

and $\delta\boldsymbol{\varepsilon}(\boldsymbol{r},t)$ corresponds to the order parameter field introduced in [1]. The Fourier expansion of the order parameter field deformed by displacement modes reads [1]

$$\delta\boldsymbol{\varepsilon}(\boldsymbol{r},t)=\sum_{\boldsymbol{k}}\delta\boldsymbol{\varepsilon}(\boldsymbol{k})\exp(i\boldsymbol{k}\cdot\boldsymbol{r})+\sum_{\boldsymbol{q},\boldsymbol{k}}\delta\boldsymbol{\varepsilon}(\boldsymbol{k}+\boldsymbol{q},t)\exp[i(\boldsymbol{k}+\boldsymbol{q})\cdot\boldsymbol{r}] \quad (40)$$

with

$$\delta\boldsymbol{\varepsilon}(\boldsymbol{k})=\delta\varepsilon_2(\boldsymbol{k})\boldsymbol{M}_2(\boldsymbol{k}) \quad (41)$$

and

$$\delta\boldsymbol{\varepsilon}(\boldsymbol{k}+\boldsymbol{q},t)=-[i\boldsymbol{u}(\boldsymbol{q},t)\cdot\boldsymbol{k}]\delta\varepsilon_2(\boldsymbol{k})\boldsymbol{M}_2(\boldsymbol{k})\ . \quad (42)$$

We remind the reader of the definition of $\boldsymbol{M}_2(\boldsymbol{k})$:

$$\boldsymbol{M}_2(\boldsymbol{k})=\boldsymbol{m}(\boldsymbol{k})\otimes\boldsymbol{m}(\boldsymbol{k})\ ,\quad \boldsymbol{m}(\boldsymbol{k})=\frac{1}{\sqrt{2}}(\boldsymbol{\xi}+i\boldsymbol{\eta})\ . \quad (43)$$

$\{\boldsymbol{\xi},\boldsymbol{\eta},\boldsymbol{k}/k\}$ is a right-handed system of orthonormal vectors and the complex vector $\boldsymbol{m}(\boldsymbol{k})$ fulfills

$$\boldsymbol{m}^*(\boldsymbol{k})\cdot\boldsymbol{m}(\boldsymbol{k})=1\quad,\quad \boldsymbol{m}(\boldsymbol{k})\cdot\boldsymbol{m}(\boldsymbol{k})=1\ . \quad (44)$$

For all calculations $\delta\varepsilon_2(\boldsymbol{k})$ is chosen real and

$$\boldsymbol{M}_2(-\boldsymbol{k})=\boldsymbol{M}^*(\boldsymbol{k})\ . \quad (45)$$

$\delta\boldsymbol{\varepsilon}(\boldsymbol{k})$ and $\delta\boldsymbol{\varepsilon}(\boldsymbol{k}+\boldsymbol{q},t)$ are responsible for the Bragg reflection and the fluctuating light intensity, respectively. Both the kinematical and the dynamical theory are only valid for small inhomogeneities $\delta\boldsymbol{\varepsilon}$. An analysis of Bragg reflection on the basis of the dynamical theory leads to [28,29]

$$\frac{\delta\varepsilon_2(\boldsymbol{k})}{\bar{\varepsilon}}\approx 0.03\ll 1\ . \quad (46)$$

A. Kinematical theory

Within the kinematical theory [25] Maxwell's equations are solved by the first-order *Born approximation* [30]. The incident light, described by the plane wave

$$\boldsymbol{E}_i(\boldsymbol{r},t)=E_0\hat{\boldsymbol{n}}_i\exp[i(\boldsymbol{k}_i\cdot\boldsymbol{r}-\omega_i t)]\quad,\quad k_i=\frac{\sqrt{\bar{\varepsilon}}}{c}\omega_i\ , \quad (47)$$

does not lose intensity when passing through the scattering medium. It only excites weak spherical waves which interfere to form the scattered light field. At a large distance r from the scattering medium the electric field appears as a plane wave with a time modulated amplitude

$$\boldsymbol{E}_s(\boldsymbol{r},t)=\frac{E_0k_f^2V}{4\pi\bar{\varepsilon}r}\delta\varepsilon_{if}(\boldsymbol{q}_s,t)\hat{\boldsymbol{n}}_f\exp[i(\boldsymbol{k}_f\cdot\boldsymbol{r}-\omega_i t)], \quad (48)$$

where

$$\delta\varepsilon_{if}(\boldsymbol{q}_s,t)=\hat{\boldsymbol{n}}_f^*\cdot\delta\boldsymbol{\varepsilon}(\boldsymbol{q}_s,t)\hat{\boldsymbol{n}}_i\ . \quad (49)$$

Scattering only occurs if there exists a Fourier coefficient for the scattering vector $\boldsymbol{q}_s$, which obeys Bragg's law:

$$\boldsymbol{q}_s=\boldsymbol{k}_f-\boldsymbol{k}_i\quad,\quad k_i=k_f\ . \quad (50)$$

The calculation of $\boldsymbol{E}_s(\boldsymbol{r},t)$ assumes that the system is embedded in a homogeneous medium with the dielectric constant $\bar{\varepsilon}$ [25]. For comparison with experiment one has to take into account the refraction of the plane waves [31] at the boundaries of the system under investigation. From Eq. (48) we obtain, for the measurable quantity, the time correlation function of the scattered electric field

$$\langle E_s^*(\boldsymbol{r},0)\,E_s(\boldsymbol{r},t)\rangle\propto\langle\delta\varepsilon_{if}^*(\boldsymbol{q}_s,0)\delta\varepsilon_{if}(\boldsymbol{q}_s,t)\rangle\times\exp(-i\omega_i t)\ . \quad (51)$$

To analyze light scattering the time correlation function of $\delta\varepsilon_{if}(\boldsymbol{q}_s,t)$ has to be considered.

The Bragg reflection from the periodic orientational pattern yields a static contribution

$$\langle\delta\varepsilon_{if}^*(\boldsymbol{k},0)\delta\varepsilon_{if}(\boldsymbol{k},t)\rangle=|\delta\varepsilon_{if}(\boldsymbol{k})|^2=|\delta\varepsilon_2(\boldsymbol{k})|^2|[\hat{\boldsymbol{n}}_i\cdot\boldsymbol{m}(\boldsymbol{k})]\,[\hat{\boldsymbol{n}}_f^*\cdot\boldsymbol{m}(\boldsymbol{k})]|^2\ . \quad (52)$$

The tensor modes of helicity $m=2$ possess a left circular polarization [32]. An investigation of Eq. (52) reveals that only light with the same polarization is reflected [33].

Light scattering from displacement modes is governed by

$$\langle\delta\varepsilon_{if}^*(\boldsymbol{k}+\boldsymbol{q},0)\delta\varepsilon_{if}(\boldsymbol{k}+\boldsymbol{q},t)\rangle=|\delta\varepsilon_{if}(\boldsymbol{k})|^2\langle[\boldsymbol{u}^*(\boldsymbol{q},0)\cdot\boldsymbol{k}]\,[\boldsymbol{u}(\boldsymbol{q},t)\cdot\boldsymbol{k}]\rangle\ . \quad (53)$$

Because of the limitation $q\ll k$ [1] we consider scattering only in the vicinity of Bragg reflection. The theory does not predict a forescattered intensity, as observed by Marcus [3] and Domberger [4], since the right-hand side of Eq. (53) vanishes for $\boldsymbol{k}=\boldsymbol{0}$. The polarization of the scattered light is determined by the first factor $|\delta\varepsilon_{if}(\boldsymbol{k})|^2$, as discussed above.

The second factor of Eq. (53) contains the time correlation function $\langle\boldsymbol{u}^*(\boldsymbol{q},t=0)\otimes\boldsymbol{u}(\boldsymbol{q},t)\rangle$ of Sec. II D

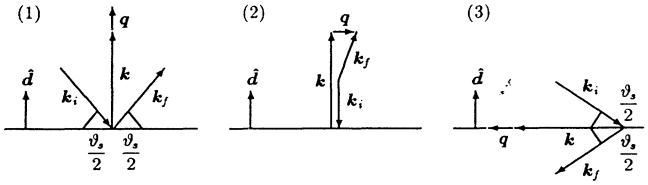

FIG. 4. Three scattering geometries to determine the dispersion relations of the longitudinal and transverse displacement modes.

TABLE I. Effective elastic constants and viscosities appearing in the measurable displacement mode of wave vector $\boldsymbol{q}$ and polarization p. The three scattering geometries (1), (2), and (3) are considered for two orientations of the blue phases relative to the cell normal $\hat{\boldsymbol{d}}$.

$\hat{\boldsymbol{d}}$	Geometry	$\boldsymbol{k}$	$\boldsymbol{q}$	p	λ_{eff}	η_{eff}
$\boldsymbol{e}_3$	(1)	$\boldsymbol{e}_3$	$\boldsymbol{e}_3$	l	$2\lambda+\lambda'+\lambda_K$	
	(2)	$\boldsymbol{e}_3$	$\cos\Phi\boldsymbol{e}_1+\sin\Phi\boldsymbol{e}_2$	t	λ	η
	(3)	$\boldsymbol{e}_3$	$\boldsymbol{e}_3$	l	$2\lambda+\lambda'+\lambda_K$	
		$(\boldsymbol{e}_1+\boldsymbol{e}_2)/\sqrt{2}$	$(\boldsymbol{e}_1+\boldsymbol{e}_2)/\sqrt{2}$	l	$2\lambda+\lambda'+\lambda_K/2$	
$(\boldsymbol{e}_1+\boldsymbol{e}_2)/\sqrt{2}$	(1)	$(\boldsymbol{e}_1+\boldsymbol{e}_2)/\sqrt{2}$	$(\boldsymbol{e}_1+\boldsymbol{e}_2)/\sqrt{2}$	l	$2\lambda+\lambda'+\lambda_K/2$	
	(2)	$(\boldsymbol{e}_1+\boldsymbol{e}_2)/\sqrt{2}$	$\boldsymbol{q}^{\text{a}}$	t	$\lambda+\cos^2\Phi\lambda_K/2$	$\eta+\cos^2\Phi\eta_K/2$
	(3)	$\boldsymbol{e}_3$	$\boldsymbol{e}_3$	l	$2\lambda+\lambda'+\lambda_K$	
		$(\boldsymbol{e}_1-\boldsymbol{e}_2)/\sqrt{2}$	$(\boldsymbol{e}_1-\boldsymbol{e}_2)/\sqrt{2}$	l	$2\lambda+\lambda'+\lambda_K/2$	

[a] $\boldsymbol{q}=\cos\Phi(\boldsymbol{e}_1-\boldsymbol{e}_2)/\sqrt{2}+\sin\Phi\boldsymbol{e}_3$.

projected onto the reciprocal wave vector $\boldsymbol{k}$. In general it depends on all three slowly relaxing modes. We intend to propose special scattering geometries which allow one to measure longitudinal and transverse modes separately. In Fig. 4 we consider three such geometries. The horizontal line symbolizes the liquid crystal cell with its normal vector $\hat{\boldsymbol{d}}$. (1) and (2) are called *Bragg* cases because the light is scattered back to the half space from which it is incident. In the *Laue* case, geometry (3), the light passes through the cell. The different dispersion relations $z(\boldsymbol{q})$ are measured by varying $\boldsymbol{q}$ via the scattering angle ϑ_s or the wavelength $2\pi/k_i$ of the incident light. In (1) and (3) $\boldsymbol{q}$ is parallel to $\boldsymbol{k}$ and for the symmetry directions of $\boldsymbol{q}$ the gradient λ_{eff}/k_P of the dispersion relation $z_l(q)$ of the longitudinal mode [Eq. (16)] can be determined. In geometry (2) transverse modes are measured at least for small wave vectors $\boldsymbol{q}$ and $z_{t2}(q)$ gives the gradient λ_{eff}/k_P and the finite frequency $\lambda_{\text{eff}}/\eta_{\text{eff}}$ [Eq. (24)]. Normally the fourfold axes c_4 of the blue phases are oriented parallel to $\hat{\boldsymbol{d}}$. In BP II $\hat{\boldsymbol{d}}\|c_2$ was also realized [4]. For these two orientations, we summarize, in Table I, the effective elastic constants and viscosities which appear in the different dispersion relations using the three scattering geometries. Note that the geometry (3) also requires an orientation perpendicular to $\hat{\boldsymbol{d}}$.

Concerning the proposed experiments, we stress three points.

(i) There are six material parameters $\lambda, \lambda', \lambda_K, \eta, \eta_K$, and k_P. From light scattering one obtains only five relative to the sixth.

(ii) All three elastic constants can be measured relative to k_P using one orientation.

(iii) The two viscosities have to be determined from transverse modes and both orientations ($\hat{\boldsymbol{d}}\|c_4$ and $\hat{\boldsymbol{d}}\|c_2$) are needed. In the BP I the second one was not observed.

A complete interpretation of Marcus's and Domberger's experiments is only possible if we understand the forescattering. This will be done in the next subsection.

B. Dynamical theory

The dynamical theory [34,35] tries to solve Maxwell's equations inside the scattering medium in a self-consistent way, taking into account the interaction between the incident and scattered waves. Then the wave field is extended to the space outside the medium via appropriate boundary conditions.

1. *Four-wave approximation*

We start with an equation of the dielectric displacement field where we assume a harmonic time dependence:

$$(\text{grad div}-\Delta)[\boldsymbol{\varepsilon}^{-1}(\boldsymbol{r})\boldsymbol{D}(\boldsymbol{r})]=\frac{\omega^2}{c^2}\boldsymbol{D}(\boldsymbol{r})\ . \tag{54}$$

Additional contributions in Eq. (54) resulting from temporal modulations of $\boldsymbol{\varepsilon}^{-1}(\boldsymbol{r},t)$ with frequencies much smaller than ω are neglected. For the small inhomogeneous part $\delta\boldsymbol{\varepsilon}(\boldsymbol{r})$ one finds

$$\boldsymbol{\varepsilon}^{-1}(\boldsymbol{r})\approx\frac{1}{\bar{\varepsilon}}\mathbf{1}-\frac{1}{\bar{\varepsilon}^2}\delta\boldsymbol{\varepsilon}(\boldsymbol{r})\ . \tag{55}$$

We consider first the undeformed orientational pattern. The differential operator of Eq. (54) possesses cubic translational symmetry and Eq. (54) is solved by a Bloch function of wave vector $\boldsymbol{k}_0'$ [36]

$$\boldsymbol{D}^{\boldsymbol{k}_0'}(\boldsymbol{r})=\sum_{\boldsymbol{k}}\boldsymbol{D}_{\boldsymbol{k}}\exp[i(\boldsymbol{k}_0'+\boldsymbol{k})\cdot\boldsymbol{r}]\quad,\quad\boldsymbol{D}_{\boldsymbol{k}}\perp\boldsymbol{k}_0'+\boldsymbol{k}\ . \tag{56}$$

With the scaled quantities

$$\boldsymbol{\psi}(\boldsymbol{k}=\boldsymbol{0})=(\bar{\varepsilon}-1)\mathbf{1} \tag{57}$$

and

$$\boldsymbol{\psi}(\boldsymbol{k}\neq\boldsymbol{0})=\frac{1}{\bar{\varepsilon}}\delta\boldsymbol{\varepsilon}(\boldsymbol{k}\neq\boldsymbol{0}) \tag{58}$$

we finally arrive at a set of linear equations for the amplitudes $\boldsymbol{D}_{\boldsymbol{k}}$, the fundamental equations of the dynamical theory

$$[-(\boldsymbol{k}_0'+\boldsymbol{k})\otimes(\boldsymbol{k}_0'+\boldsymbol{k})+|\boldsymbol{k}_0'+\boldsymbol{k}|^2\mathbf{1}] \times\sum_{\boldsymbol{k}'}\boldsymbol{\varepsilon}^{-1}(\boldsymbol{k}-\boldsymbol{k}')\,\boldsymbol{D}_{\boldsymbol{k}'}=\frac{\omega^2}{c^2}\,\boldsymbol{D}_{\boldsymbol{k}}\ . \tag{59}$$

$k_0=\sqrt{\bar{\varepsilon}}\omega/c$ is the wave number of light traveling with frequency ω in a homogeneous medium of dielectric constant $\bar{\varepsilon}$.

The Bloch function $\boldsymbol{D}^{\boldsymbol{k}_0'}(\boldsymbol{r})$ consists of a sum of plane waves. In the case of light scattering the wave vector $\boldsymbol{k}_0'$ belongs to the incident light, while the others describe scattered waves. We are only interested in the wave vector range close to Bragg reflections. The kinematical theory correctly describes their position by Bragg's law (50), but not their intensities. In the Bloch function (56) we therefore consider merely wave vectors which nearly satisfy Bragg's law. The dimension of the set of fundamental equations (59) is reduced considerably.

Figure 5 shows the scattering geometry of the experiments of Marcus [3] and Domberger [4], which we will study in the following. The cubic blue phase is enclosed in a liquid crystal cell with boundaries at $z=0$ and d. The wave vector of the incident light is $\boldsymbol{k}_0/\sqrt{\bar{\varepsilon}}$. Besides the usual refraction, governed by $\bar{\varepsilon}$, the dynamical theory takes into account an additional refractive index $1+\delta_0$ due to the inhomogeneity of $\boldsymbol{\varepsilon}(\boldsymbol{r},t)$:

$$\boldsymbol{k}_0'=(1+\delta_0)\boldsymbol{k}_0\quad,\quad \delta_0\ll 1\ . \tag{60}$$

Because the inhomogeneities $\delta\boldsymbol{\varepsilon}$ in the dielectric tensor are small, δ_0 is small too.

We solve Eq. (59) by the ansatz

$$\boldsymbol{D}^{\boldsymbol{k}_0'}(\boldsymbol{r})=\boldsymbol{D}_0\exp[i\boldsymbol{k}_0'\cdot\boldsymbol{r}]+\boldsymbol{D}_{\boldsymbol{k}}\exp[i(\boldsymbol{k}_0'+\boldsymbol{k})\cdot\boldsymbol{r}] +\boldsymbol{D}_{\boldsymbol{k}+\boldsymbol{q}}\exp[i(\boldsymbol{k}_0'+\boldsymbol{k}+\boldsymbol{q})\cdot\boldsymbol{r}] +\boldsymbol{D}_{\boldsymbol{q}}\exp[i(\boldsymbol{k}_0'+\boldsymbol{q})\cdot\boldsymbol{r}]\ , \tag{61}$$

the *four-wave approximation*. The third plane wave describes the scattering from a displacement mode. In the above discussion we had restricted ourselves to the undeformed orientational pattern because the displacement modes destroy the translational symmetry and the Bloch function (56) cannot be chosen as a solution of Eq. (54). On the other hand, this third contribution appears in the kinematical theory and we will take it into account by the amplitude $\boldsymbol{\psi}(\boldsymbol{k}+\boldsymbol{q})$ in the fundamental equations (59). We consider only one displacement mode, i.e., we neglect the coupling between light scattering from different modes. The fourth plane wave describes the forescattering with an effective scattering vector $\boldsymbol{q}$. It can be justified by two double scattering processes illustrated in Fig. 6. The single scattering events have to fulfill Bragg's law only approximately. In the second process the wave vector $-(\boldsymbol{k}-\boldsymbol{q})$ is involved and we must also use the amplitude $\boldsymbol{\psi}[-(\boldsymbol{k}-\boldsymbol{q})]$ in the following.

We insert the ansatz (61) into the fundamental equations (59), choose all Fourier coefficients besides $\boldsymbol{\psi}(\pm\boldsymbol{k})$ and $\boldsymbol{\psi}[\pm(\boldsymbol{k}\pm\boldsymbol{q})]$ zero, and get four vector equations

$$-k_0^2\,2\delta_0\,\boldsymbol{D}_0=[\boldsymbol{k}_0'\otimes\boldsymbol{k}_0'-|\boldsymbol{k}_0'|^2\mathbf{1}] \times\{\boldsymbol{\psi}(-\boldsymbol{k})\,\boldsymbol{D}_{\boldsymbol{k}}+\boldsymbol{\psi}[-(\boldsymbol{k}+\boldsymbol{q})]\,\boldsymbol{D}_{\boldsymbol{k}+\boldsymbol{q}}\}, \tag{62}$$

$$-k_0^2\,(\alpha_1-2\delta_0)\,\boldsymbol{D}_{\boldsymbol{k}}=[(\boldsymbol{k}_0'+\boldsymbol{k})\otimes(\boldsymbol{k}_0'+\boldsymbol{k})-|\boldsymbol{k}_0'+\boldsymbol{k}|^2\mathbf{1}] \times[\boldsymbol{\psi}(\boldsymbol{k})\,\boldsymbol{D}_0+\boldsymbol{\psi}(\boldsymbol{k}-\boldsymbol{q})\,\boldsymbol{D}_{\boldsymbol{q}}], \tag{63}$$

$$-k_0^2\,(\alpha_2-2\delta_0)\,\boldsymbol{D}_{\boldsymbol{k}+\boldsymbol{q}} =[(\boldsymbol{k}_0'+\boldsymbol{k}+\boldsymbol{q})\otimes(\boldsymbol{k}_0'+\boldsymbol{k}+\boldsymbol{q})-|\boldsymbol{k}_0'+\boldsymbol{k}+\boldsymbol{q}|^2\mathbf{1}] \times[\boldsymbol{\psi}(\boldsymbol{k}+\boldsymbol{q})\,\boldsymbol{D}_0+\boldsymbol{\psi}(\boldsymbol{k})\,\boldsymbol{D}_{\boldsymbol{q}}], \tag{64}$$

$$-k_0^2\,(\alpha_3+2\delta_0)\,\boldsymbol{D}_{\boldsymbol{q}} =[(\boldsymbol{k}_0'+\boldsymbol{q})\otimes(\boldsymbol{k}_0'+\boldsymbol{q})-|\boldsymbol{k}_0'+\boldsymbol{q}|^2\mathbf{1}] \times\{\boldsymbol{\psi}[-(\boldsymbol{k}-\boldsymbol{q})]\,\boldsymbol{D}_{\boldsymbol{k}}+\boldsymbol{\psi}(-\boldsymbol{k})\,\boldsymbol{D}_{\boldsymbol{k}+\boldsymbol{q}}\}\ . \tag{65}$$

In the left-hand sides of the equations only the lowest orders in q/k and δ_0 and $\boldsymbol{k}\approx-2\boldsymbol{k}_0$ have been taken into account. The introduced quantities

$$\alpha_1=(2\boldsymbol{k}_0\cdot\boldsymbol{k}+\boldsymbol{k}^2)/k_0^2\ , \tag{66}$$

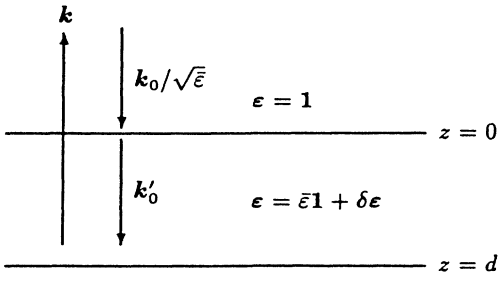

FIG. 5. Scattering geometry of Marcus [3] and Domberger [4].

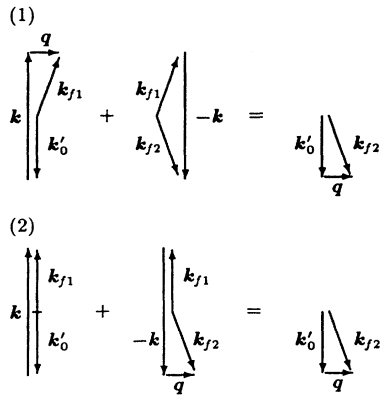

FIG. 6. Double scattering processes to explain the forescattering with an effective scattering vector $\boldsymbol{q}$.

$$\alpha_2 = [2\boldsymbol{k}_0 \cdot (\boldsymbol{k}+\boldsymbol{q}) + (\boldsymbol{k}+\boldsymbol{q})^2]/k_0^2, \tag{67}$$

and

$$\alpha_3 = (2\boldsymbol{k}_0 \cdot \boldsymbol{q} + \boldsymbol{q}^2)/k_0^2 \tag{68}$$

vanish if $\boldsymbol{k}_0$ and the scattering vectors $\boldsymbol{k}$, $\boldsymbol{k}+\boldsymbol{q}$, or $\boldsymbol{q}$ fulfill Bragg's law. The free parameter δ_0 is determined by the claim that we have a nontrivial solution. In general there are eight different values possible, so that each scattering vector in the ansatz (61) is represented by a *bundle* of eight plane waves.

2. *Determination of the light-scattering intensities*

From Eqs. (41), (42), and (58) we get

$$\boldsymbol{\psi}(\boldsymbol{k}) = \psi(\boldsymbol{k})\, \boldsymbol{M}_2(\boldsymbol{k}), \quad \psi(\boldsymbol{k}) = \frac{1}{\bar{\varepsilon}}\, \delta\varepsilon_2(\boldsymbol{k}), \tag{69}$$

and

$$\boldsymbol{\psi}(\boldsymbol{k}+\boldsymbol{q}) = \psi(\boldsymbol{k}+\boldsymbol{q})\, \boldsymbol{M}_2(\boldsymbol{k}) \tag{70}$$

with

$$\psi(\boldsymbol{k}+\boldsymbol{q}) = -i\boldsymbol{u}(\boldsymbol{q}) \cdot \boldsymbol{k}\, \psi(\boldsymbol{k}) \ . \tag{71}$$

Introduction of new scaled quantities leads to

$$\frac{\delta_0}{2|\psi(\boldsymbol{k})|} \longrightarrow \delta_0 \ , \quad \frac{\alpha_i}{2|\psi(\boldsymbol{k})|} \longrightarrow \alpha_i \ , \tag{72}$$

$$\frac{\psi(\boldsymbol{k})}{|\psi(\boldsymbol{k})|} = \gamma \quad , \quad \gamma = 1 \text{ or } -1 \tag{73}$$

and

$$\frac{\psi(\boldsymbol{k}+\boldsymbol{q})}{|\psi(\boldsymbol{k})|} = \varepsilon_1 \quad , \quad \varepsilon_1 = -i\gamma \boldsymbol{u}(\boldsymbol{q}) \cdot \boldsymbol{k} \ . \tag{74}$$

An important parameter will be

$$\varepsilon = |\varepsilon_1| = |\boldsymbol{u}(\boldsymbol{q}) \cdot \boldsymbol{k}| \ . \tag{75}$$

The wave vector $\boldsymbol{k}$ gives a preferred direction of the scattering geometry. We use the complex unit vector $\boldsymbol{m}(\boldsymbol{k})$ from Eqs. (43) to introduce

$$\boldsymbol{D}_0 = D_{01}\, \boldsymbol{m}^*(\boldsymbol{k}) + D_{0-1}\, \boldsymbol{m}(\boldsymbol{k}) \tag{76}$$

and

$$\boldsymbol{D}_{\boldsymbol{k}} = D_{\boldsymbol{k}1}\, \boldsymbol{m}(\boldsymbol{k}) + D_{\boldsymbol{k}-1}\, \boldsymbol{m}^*(\boldsymbol{k}) \ . \tag{77}$$

The first components describe left and the second components right circularly polarized light waves.

From Eqs. (62) and (63) follow the relations

$$\delta_0 D_{0-1} = 0, \qquad (\alpha_1 - 2\delta_0) D_{\boldsymbol{k}-1} = 0 \ , \tag{78}$$

where Eqs. (43) – (45) have been used. According to the first equation, right circularly polarized light does not interact with the inhomogeneous medium ($\delta_0 = 0 \leftrightarrow \boldsymbol{k}_0' = \boldsymbol{k}_0$). Due to the boundary conditions (see below) $D_{\boldsymbol{k}-1}$ always vanishes and the Bragg reflected light is left circularly polarized, as we have already seen in Sec. III A. The remaining six equations are

$$\begin{pmatrix}
\boxed{\begin{matrix} \frac{\varepsilon_1^*}{2} & \frac{\gamma}{2} & 0 & -2\delta_0 \\ 0 & -\alpha_1 + 2\delta_0 & -\frac{\varepsilon_1^*}{2} & \frac{\gamma}{2} \\ -\alpha_2 + 2\delta_0 & 0 & \frac{\gamma}{2} & \frac{\varepsilon_1}{2} \\ \frac{\gamma}{2} & -\frac{\varepsilon_1}{2} & -\alpha_3 - 2\delta_0 & 0 \end{matrix}} & \begin{matrix} 0 & 0 \\ 0 & 0 \\ 0 & 0 \\ 0 & 0 \end{matrix} \\
\begin{matrix} 0 & 0 \\ \gamma\left(\boldsymbol{m}^*(\boldsymbol{k}) \cdot \frac{\boldsymbol{q}}{k}\right)^2 & -\varepsilon_1\left(\boldsymbol{m}^*(\boldsymbol{k}) \cdot \frac{\boldsymbol{q}}{k}\right)^2 \end{matrix} & \begin{matrix} \gamma\left(\boldsymbol{m}(\boldsymbol{k}) \cdot \frac{\boldsymbol{q}}{k}\right)^2 & \varepsilon_1\left(\boldsymbol{m}(\boldsymbol{k}) \cdot \frac{\boldsymbol{q}}{k}\right)^2 \\ 0 & 0 \end{matrix} & \begin{matrix} \frac{\alpha_2}{2} - \delta_0 & 0 \\ 0 & \frac{\alpha_3}{2} + \delta_0 \end{matrix}
\end{pmatrix}
\begin{pmatrix}
\boldsymbol{m}^*(\boldsymbol{k}) \cdot \boldsymbol{D}_{\boldsymbol{k}+\boldsymbol{q}} \\ D_{\boldsymbol{k}1} \\ \boldsymbol{m}(\boldsymbol{k}) \cdot \boldsymbol{D}_{\boldsymbol{q}} \\ D_{01} \\ \boldsymbol{m}(\boldsymbol{k}) \cdot \boldsymbol{D}_{\boldsymbol{k}+\boldsymbol{q}} \\ \boldsymbol{m}^*(\boldsymbol{k}) \cdot \boldsymbol{D}_{\boldsymbol{q}}
\end{pmatrix} = \boldsymbol{0} . \tag{79}$$

A nontrivial solution needs a vanishing determinant of the framed matrix. For each set of parameters α_i and ε_1, the four zeros $\delta_0^{(i)}$ were calculated via the exact formula, which was implemented in a FORTRAN program. The amplitudes follow from Eqs. (79):

$$D_{\boldsymbol{k}1}^{(i)} = x_{\boldsymbol{k}}^{(i)} D_{01}^{(i)} = -2\gamma\, \frac{\alpha_3}{n_2^{(i)}}\, D_{01}^{(i)} \ , \tag{80}$$

$$\boldsymbol{m}^*(\boldsymbol{k}) \cdot \boldsymbol{D}_{\boldsymbol{k}+\boldsymbol{q}}^{(i)} = x_{\boldsymbol{k}+\boldsymbol{q}}^{(i)} D_{01}^{(i)} = -\varepsilon_1\, \frac{z_{\boldsymbol{k}+\boldsymbol{q}}^{(i)}}{n_1^{(i)} n_2^{(i)}}\, D_{01}^{(i)}, \tag{81}$$

and

$$\boldsymbol{m}(\boldsymbol{k}) \cdot \boldsymbol{D}_{\boldsymbol{q}}^{(i)} = x_{\boldsymbol{q}}^{(i)} D_{01}^{(i)} = \gamma\varepsilon_1\, \frac{z_{\boldsymbol{q}}^{(i)}}{n_1^{(i)} n_2^{(i)}}\, D_{01}^{(i)}, \tag{82}$$

where we use the abbreviations

$$n_1^{(i)} = 1 + 4(\alpha_3 + 2\delta_0^{(i)})\,(-\alpha_2 + 2\delta_0^{(i)}) \ , \tag{83}$$

$$n_2^{(i)} = 1 + \varepsilon^2 + 4(\alpha_3 + 2\delta_0^{(i)})\,(-\alpha_1 + 2\delta_0^{(i)}) \ , \tag{84}$$

$$z_{\boldsymbol{k}+\boldsymbol{q}}^{(i)} = 2[\alpha_3 + (\alpha_3 + 2\delta_0^{(i)})n_2^{(i)}], \tag{85}$$

and

$$z_{\boldsymbol{q}}^{(i)} = 4\alpha_3(-\alpha_2 + 2\delta_0^{(i)}) - n_2^{(i)} \ . \tag{86}$$

The amplitudes $\boldsymbol{m}(\boldsymbol{k})\cdot\boldsymbol{D}(\boldsymbol{k}+\boldsymbol{q})$ and $\boldsymbol{m}^*(\boldsymbol{k})\cdot\boldsymbol{D}(\boldsymbol{q})$ vanish for $2\delta_0 = \alpha_2$ and $2\delta_0 = -\alpha_3$, respectively, due to the boundary conditions. Otherwise they are a factor $(q/k)^2$ smaller than the corresponding amplitudes $\boldsymbol{m}^*(\boldsymbol{k})\cdot\boldsymbol{D}(\boldsymbol{k}+\boldsymbol{q})$ and $\boldsymbol{m}(\boldsymbol{k})\cdot\boldsymbol{D}(\boldsymbol{q})$ and can be neglected. Hence the scattered light is nearly left circularly polarized.

The bundles of plane waves of the different light rays in the medium are the incident light ray

$$\exp(-i\omega t + ik_0 z)\sum_{i=1}^{4} D_{01}^{(i)} \exp[ik_0\delta_0^{(i)}z]\,\boldsymbol{m}^*(\boldsymbol{k}) \ , \tag{87}$$

the light ray with scattering vector $\boldsymbol{k}$

$$\exp[-i\omega t + i(k_0 - k)z]\sum_{i=1}^{4} D_{\boldsymbol{k}1}^{(i)} \exp[ik_0\delta_0^{(i)}z]\,\boldsymbol{m}(\boldsymbol{k}) \ , \tag{88}$$

the light ray with scattering vector $\boldsymbol{k}+\boldsymbol{q}$

$$\exp[-i\omega t + i(k_0 - k)z + i\boldsymbol{q}\cdot\boldsymbol{r}]$$

$$\times\sum_{i=1}^{4} \boldsymbol{m}^*(\boldsymbol{k})\cdot\boldsymbol{D}_{\boldsymbol{k}+\boldsymbol{q}}^{(i)} \exp[ik_0\delta_0^{(i)}z]\,\boldsymbol{m}(\boldsymbol{k}) \ , \tag{89}$$

and the light ray with scattering vector $\boldsymbol{q}$

$$\exp[-i\omega t + ik_0 z + i\boldsymbol{q}\cdot\boldsymbol{r}]$$

$$\times\sum_{i=1}^{4} \boldsymbol{m}(\boldsymbol{k})\cdot\boldsymbol{D}_{\boldsymbol{q}}^{(i)} \exp[ik_0\delta_0^{(i)}z]\,\boldsymbol{m}^*(\boldsymbol{k}) \ . \tag{90}$$

The four still unknown amplitudes $D_{01}^{(i)}$ are determined from boundary conditions.

1. *The incident wave.* The incident wave outside the scattering medium with the relevant polarization is

$$\boldsymbol{E}_0(\boldsymbol{r},t) = E_0\boldsymbol{m}^*(\boldsymbol{k})\,\exp(-i\omega t + ik_0 z/\sqrt{\bar{\varepsilon}}) \ . \tag{91}$$

At $z = 0$ it has to change into the bundle of Eq. (87) where the tangential component of the electric field must be continuous:

$$\sum_{i=1}^{4} D_{01}^{(i)} = \bar{\varepsilon}E_0 \ . \tag{92}$$

The inhomogeneity $\delta\boldsymbol{\varepsilon}(\boldsymbol{r},t)$ is neglected.

2. *The Bragg case.* The bundles (88) and (89) of the scattering vectors $\boldsymbol{k}$ and $\boldsymbol{k}+\boldsymbol{q}$ have to vanish at $z = d$ because they are scattered back in the half space $z < 0$:

$$\sum_{i=1}^{4} D_{\boldsymbol{k}1}^{(i)} c_i = 0 \tag{93}$$

and

$$\sum_{i=1}^{4} \boldsymbol{m}^*(\boldsymbol{k})\cdot\boldsymbol{D}_{\boldsymbol{k}+\boldsymbol{q}}^{(i)} c_i = 0 \ . \tag{94}$$

Here we have introduced

$$c_i = \exp[i4A\delta_0^i] \tag{95}$$

with the *optical thickness*

$$A = k_0 d|\psi(\boldsymbol{k})|/2 \ . \tag{96}$$

The kinematical theory is valid for $A \ll 1$ [35].

3. *The Laue case.* The bundle (90) of scattering vector $\boldsymbol{q}$ has to vanish at $z = 0$:

$$\sum_{i=1}^{4} \boldsymbol{m}(\boldsymbol{k})\cdot\boldsymbol{D}_{\boldsymbol{q}}^{(i)} = 0 \ . \tag{97}$$

Using Eqs. (80) – (82) we finally get an inhomogeneous system of four linear equations with the solutions

$$D_{01}^{(l)} = \frac{\varepsilon_{lijk}\,x_{\boldsymbol{q}}^{(i)}x_{\boldsymbol{k}}^{(j)}x_{\boldsymbol{k}+\boldsymbol{q}}^{(k)}c_j c_k}{\sum_l \varepsilon_{lijk}\,x_{\boldsymbol{q}}^{(i)}x_{\boldsymbol{k}}^{(j)}x_{\boldsymbol{k}+\boldsymbol{q}}^{(k)}c_j c_k}\,\bar{\varepsilon}E_0 \tag{98}$$

(Einstein's summation convention is assumed). ε_{ijkl} denotes the permutation symbol in four dimensions:

$$\varepsilon_{ijkl} = \begin{cases} 1, & \text{even permutations of } 1\,2\,3\,4 \\ -1, & \text{odd permutations of } 1\,2\,3\,4 \\ 0, & \text{other cases} \ . \end{cases} \tag{99}$$

For the calculation of the light scattering intensities we have to know how the bundles appear outside the scattering medium. The single plane waves fulfill two conditions: (i) the tangential component of a wave vector behaves continuously at the boundary [34,37] and (ii) outside the medium $\delta_0^{(i)}$ vanishes and $\boldsymbol{k}_0'$ has to be replaced by $\boldsymbol{k}_0/\sqrt{\bar{\varepsilon}}$. Hence a bundle of plane waves merges into one. Its amplitude is calculated as a sum of the single amplitudes weighted by the factors $\exp[ik_0\delta_0^{(i)}z]$, where the boundary conditions of the electric field also have to be considered. z is the coordinate of the boundary. We refer all light-scattering intensities to the intensity $I_0 = |E_0|^2$ of the incident light and get for the scattering vector $\boldsymbol{k}$

$$\frac{I_{\boldsymbol{k}}}{I_0} = \left|\frac{\sum_l D_{\boldsymbol{k}1}^{(l)}}{\bar{\varepsilon}E_0}\right|^2 = \left|\frac{\varepsilon_{lijk}\,z_{\boldsymbol{k}}n_1^{(l)}z_{\boldsymbol{q}}^{(i)}n_1^{(j)}z_{\boldsymbol{k}+\boldsymbol{q}}^{(k)}c_j c_k}{\varepsilon_{lijk}\,n_1^{(l)}n_2^{(l)}z_{\boldsymbol{q}}^{(i)}n_1^{(j)}z_{\boldsymbol{k}+\boldsymbol{q}}^{(k)}c_j c_k}\right|^2 , \tag{100}$$

the scattering vector $\boldsymbol{k}+\boldsymbol{q}$

$$\frac{I_{k+q}}{I_0} = \left| \frac{\sum_l \boldsymbol{m}^*(\boldsymbol{k}) \cdot \boldsymbol{D}^{(l)}_{k+q}}{\bar{\varepsilon} E_0} \right|^2 = \varepsilon^2 \left| \frac{\varepsilon_{lijk}\, z^{(l)}_{k+q} z^{(i)}_{q} n^{(j)}_1 z^{(k)}_{k+q} c_j c_k}{\varepsilon_{lijk}\, n^{(l)}_1 n^{(l)}_2 z^{(i)}_{q} n^{(j)}_1 z^{(k)}_{k+q} c_j c_k} \right|^2 , \quad (101)$$

and the scattering vector $\boldsymbol{q}$

$$\frac{I_q}{I_0} = \left| \frac{\sum_l c_l\, \boldsymbol{m}(\boldsymbol{k}) \cdot \boldsymbol{D}^{(l)}_{q}}{\bar{\varepsilon} E_0} \right|^2 = \varepsilon^2 \left| \frac{\varepsilon_{lijk}\, c_l z^{(l)}_{q} z^{(i)}_{q} n^{(j)}_1 z^{(k)}_{k+q} c_j c_k}{\varepsilon_{lijk}\, n^{(l)}_1 n^{(l)}_2 z^{(i)}_{q} n^{(j)}_1 z^{(k)}_{k+q} c_j c_k} \right|^2 . \quad (102)$$

3. Discussion

What are the appropriate variables for discussing the calculated intensities? α_1 is a measure for the deviation of the wavelength $\lambda = 2\pi/k_0$ of the incident light from the Bragg wavelength $\lambda_B = \pi/k$:

$$\alpha_1 \approx 4 \left(1 - 2\frac{k_0}{k}\right) \frac{1}{2|\psi(\boldsymbol{k})|} \approx 4 \frac{\lambda - \lambda_B}{\lambda_B} \frac{1}{2|\psi(\boldsymbol{k})|} . \quad (103)$$

One task will be to determine the wave vector $\boldsymbol{q}$ of the displacement mode which contributes most to the light scattering intensities I_{k+q} and I_q. We choose the components of $\boldsymbol{q}$ parallel and perpendicular to the z direction: q_3 and $q_\perp$. Neglecting the small variations of λ, a constant $q_\perp$ is equivalent to a constant scattering angle. In the following pictures we therefore fix $q_\perp$ and show the intensity dependence on α_1 and q_3. The components used are in scaled units

$$\frac{q_3}{k} \frac{1}{2|\psi(\boldsymbol{k})|} \longrightarrow q_3 \quad , \quad \frac{q_\perp}{k} \frac{1}{2|\psi(\boldsymbol{k})|} \longrightarrow q_\perp \quad (104)$$

and the scaled α_2 and α_3 are given by

$$\alpha_2 \approx -4q_3 + \alpha_1 + |\psi(\boldsymbol{k})|(8q^2 - 6\alpha_1 q_3 + \alpha_1^2) , \quad (105)$$

$$\alpha_3 \approx 4q_3 + 2|\psi(\boldsymbol{k})|(4q^2 + \alpha_1 q_3) . \quad (106)$$

For the discussion we use one set of parameters. Usual values for the thickness d and the lateral extension l of the platelets of cubic blue phases are [4]

$$d = 12\ \mu\text{m} \quad , \quad l = 30\ \mu\text{m} . \quad (107)$$

We choose the lattice constant

$$b = 0.2\ \mu\text{m} \longrightarrow k = \frac{2\pi}{b} = 31.42\ \mu\text{m}^{-1} \quad (108)$$

and take the amplitude $\psi(\boldsymbol{k})$ according to experiment [28,29]

$$|\psi(\boldsymbol{k})| = 0.0265 \longrightarrow A = 2.5 . \quad (109)$$

The fluctuating quantity $\varepsilon = |\boldsymbol{u}(\boldsymbol{q}) \cdot \boldsymbol{k}|$ follows from Eq. (34) where the anisotropy and the different polarizations are neglected:

$$\varepsilon(q_\perp, q_3) = \varepsilon_0 \frac{q_0}{q} \quad , \quad \varepsilon_0 = \left(\frac{k_B T}{V} \frac{k^2}{\lambda_{\text{eff}} q_0^2} \right)^{1/2} \approx 0.02 . \quad (110)$$

We have chosen $q_0 = \pi/l$, $V = dl^2$, $\lambda_{\text{eff}} = 1000$ ergs/cm^3, and $T = 300$ K ($k_B = 1.38 \times 10^{-16}$ ergs/K). The finite extension of the platelets does not allow wave vectors whose components q_3 and $q_\perp$ are both situated in $[-\pi/d, \pi/d]$ and $[-\pi/l, \pi/l]$, respectively. Whenever this occurs we set I_{k+q} and I_q equal to zero. The intensities will be discussed for $q_\perp = 0.02$, 1.00, 1.50, and 3.00. In unscaled units the values correspond to $q_\perp/k = 10^{-3}$, 0.053, 0.080, and 0.160. They cover the range used by Marcus [3].

Figure 7 shows a three-dimensional representation of I_k and its contour plot for $q_\perp = 0.1$. Only in the vicinity of $q_3 = 0$ does the intensity decrease slightly, due to the light scattering from displacement modes. For constant

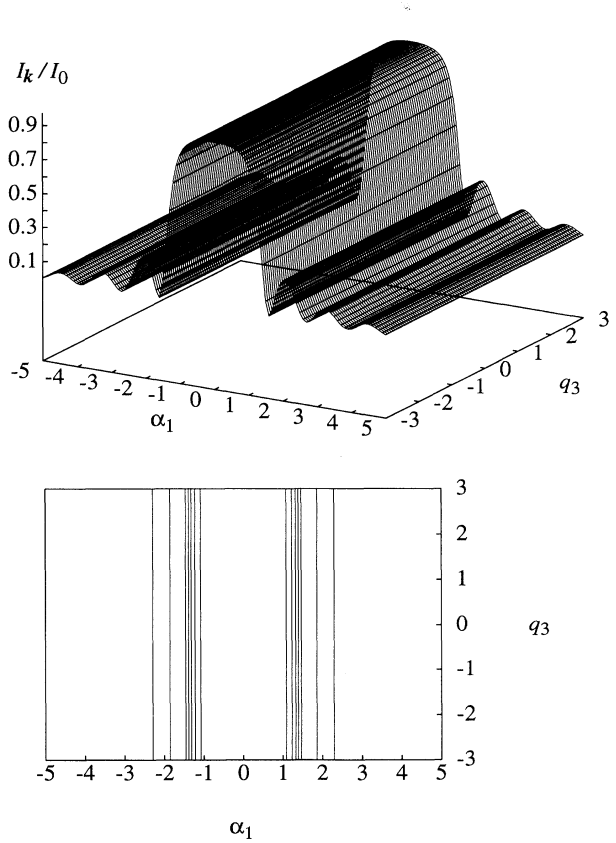

FIG. 7. Three-dimensional representation and a contour plot of the light-scattering intensity I_k relative to I_0 depending on α_1 and q_3: $q_\perp = 0.1$.

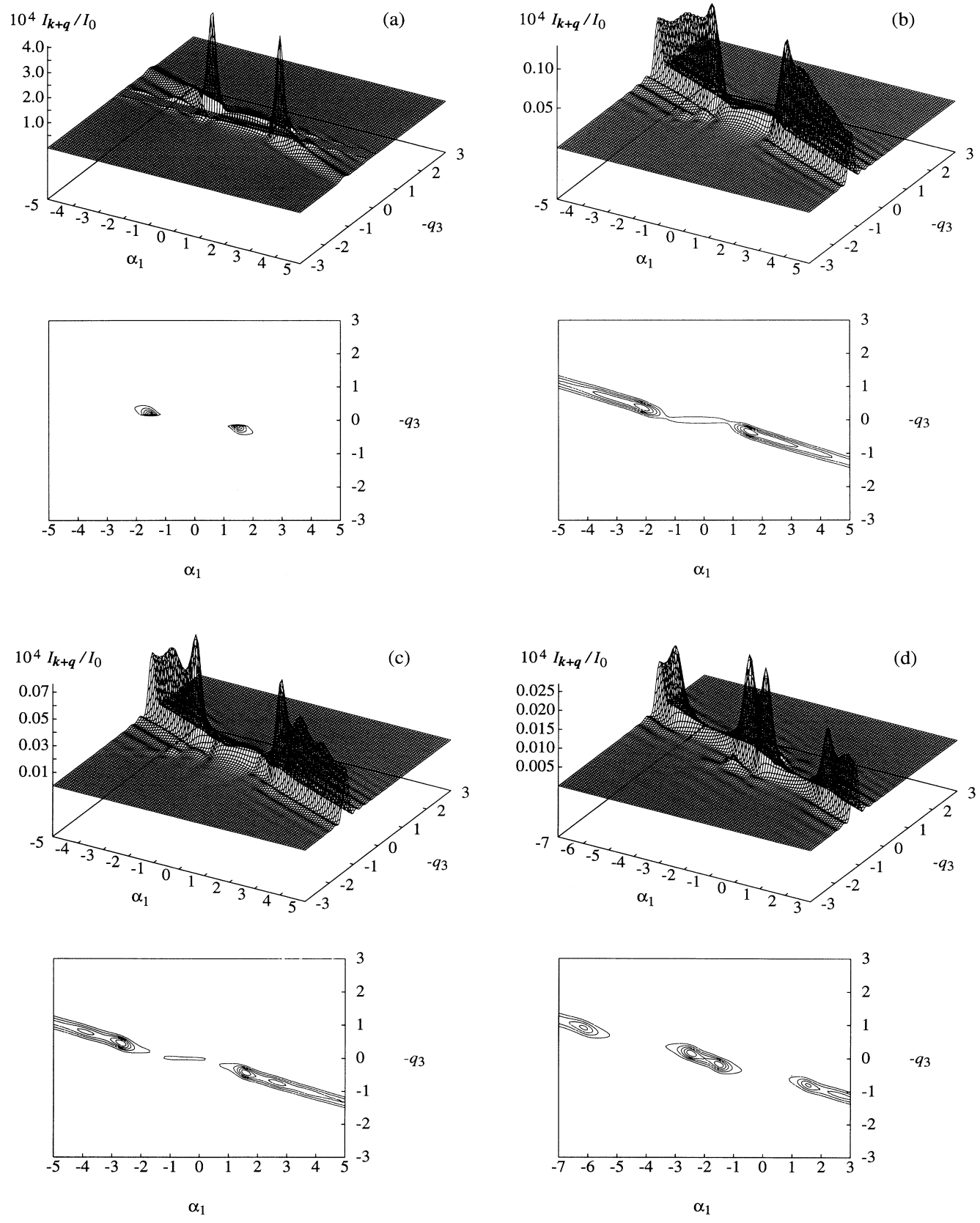

FIG. 8. Three-dimensional representation and a contour plot of the light-scattering intensities I_{k+q} relative to I_0 depending on α_1 and q_3: (a) $q_\perp = 0.02$, (b) $q_\perp = 1.00$, (c) $q_\perp = 1.50$, and (d) $q_\perp = 3.00$.

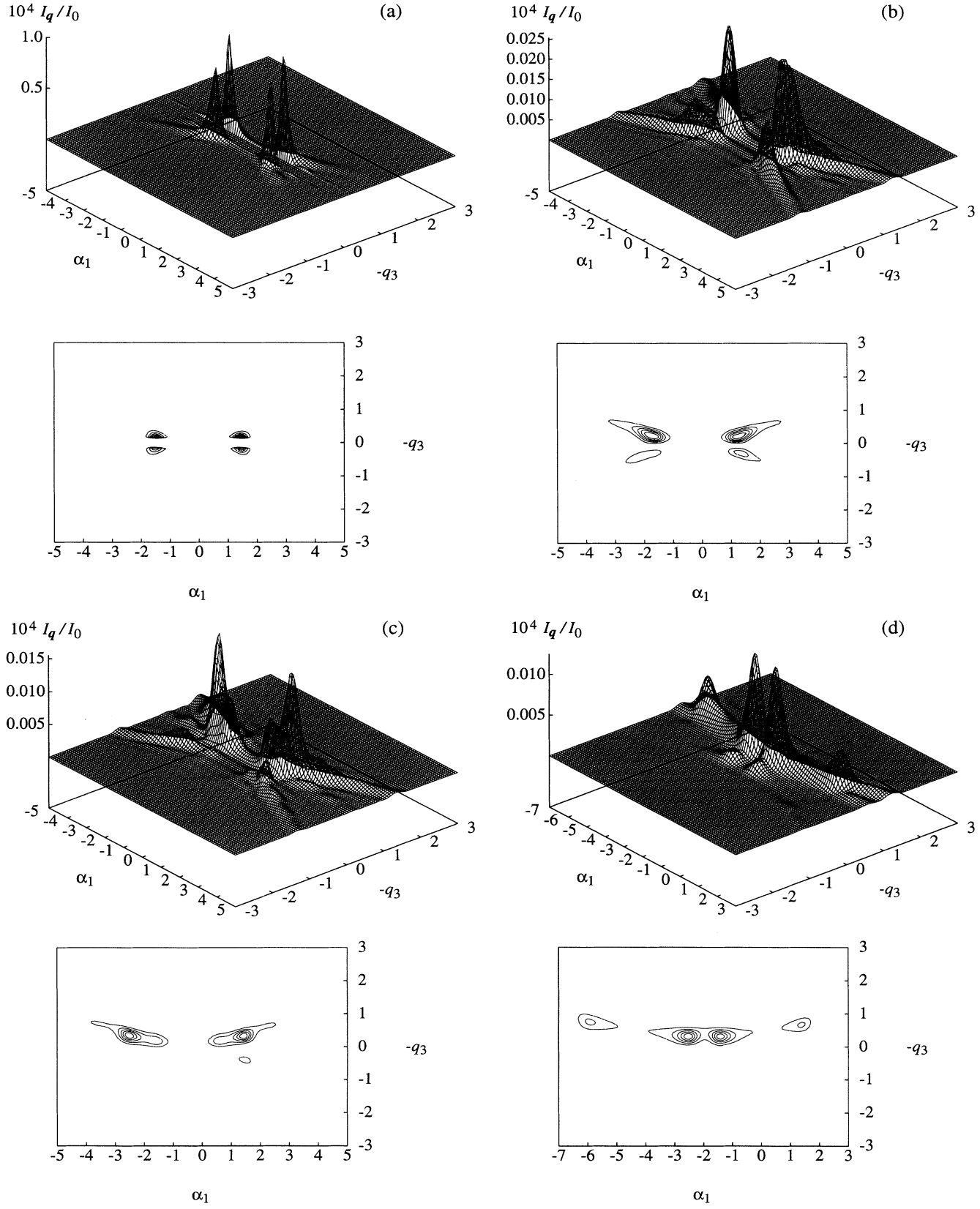

FIG. 9. Three-dimensional representation and a contour plot of the light-scattering intensities I_q relative to I_0 depending on α_1 and q_3: (a) $q_\perp = 0.02$, (b) $q_\perp = 1.00$, (c) $q_\perp = 1.50$, and (d) $q_\perp = 3.00$.

q_3 the typical curve of a two-wave approximation is seen [35]. Note that the intensity of the Bragg reflection is nearly one. From the experiments we know that the edges of the Bragg band are important. Here they are situated at $\alpha_1 = \pm 1.5$.

We have studied I_{k+q}/ε^2 and I_q/ε^2 for different $\varepsilon < 0.1$ and found that they only weakly depend on ε. This can be understood from the following consideration. Usually the small quantity ε^2 can be neglected. Only in one term in the determinant of the framed matrix in Eq. (79) is this not possible. As a result, we may replace the factor ε^2 in Eqs. (101) and (102) by $\langle \varepsilon_1^*(t)\,\varepsilon_1(0) \rangle$. The same time correlation function appeared in the kinematical theory [Eq. (53)] and therefore all statements about the measurement of dispersion relations remain valid.

Figure 8 represents the intensities I_{k+q} for the four different components $q_\perp$. I_{k+q} differs from zero only in a narrow range of q_3. The location of the maximum for constant α_1 follows qualitatively from Bragg's law. The figure with $q_\perp = 0.02$ contains two sharp peaks at $q_3 \approx 0$ and $\alpha_1 = \pm 1.5$, i.e., at the edges of the Bragg band. This is exactly what Marcus saw in his first experiments [2]. But our calculated intensity is still a factor 100 smaller. It becomes larger for decreasing elastic constants and for an increasing thickness d [Eq. (110)]. In the last case the finitely extended system allows smaller wave numbers q. Also the optical thickness A and therefore the scattering power of the system increases with d. The strong decay of I_{k+q} for $|\alpha_1| > 1.5$ depends on the $1/q$ behavior of ε [Eq. (110)]. At larger $q_\perp$, the right maximum remains at $\alpha_1 \approx 1.5$ and the left one moves to smaller values of α_1. Finally there appear two additional maxima in the expanding valley. At last we judge the scattering geometries given in Fig. 4. In the first one, we have to choose $\vartheta_s = 180°$ for a comparison with our calculations. $q_\perp$ is zero and from Fig. 8(a) we realize that the variation of the light wavelength λ "stimulates" different q_3, but they do not exactly obey Bragg's law. Geometry (2) corresponds to $\alpha_1 = 0$ and the scattering intensities are small. To increase them one has to change α_1, but then the wave vector $\boldsymbol{q}$ possesses a general direction and a superposition of all three displacement modes is measured.

Figure 9 shows the intensities I_q. For $q_\perp = 0.02$ four sharp peaks exist at $\alpha_1 \approx \pm 1.5$ and $q_3 \approx \pm 0.15$. In the contour plot the maxima at the top left and at the bottom right can be identified with the first double scattering process of Fig. 6, because the scattering vector $\boldsymbol{k} + \boldsymbol{q}$ best satisfies Bragg's law. The third and fourth maxima belong to the second process. The peaks with negative q_3 vanish for increasing $q_\perp$. The others expand and two new maxima appear. Again the maximum at $\alpha_1 \approx 1.5$ does not move and the whole contour lines shift to the left. A maximum is always present at $\alpha_1 = -1.5$. The forescattering experiments also show these large scattering intensities at the edges of the Bragg reflection [3,4]. However, our calculations imply that the situation is more complicated. Finally we are able to judge the frequencies measured by Marcus [3]. We concentrate on Figs. 9(a) and 9(b). The maxima lie symmetrically about $q_3 = 0$. Because of the cubic point symmetry, the wave vectors $\boldsymbol{q}$ are equivalent. But they possess a general direction and all three slow relaxing displacement modes should be seen. Two of them show the behavior of the transverse modes. Their "finite" frequencies $\lambda_{\text{eff}}/\eta_{\text{eff}}$ correspond to the two measured ones. The frequencies of Marcus [3] differ by a factor 3. We can explain this factor from $\lambda_{\text{eff}}/\eta_{\text{eff}}$ only if we assume a large anisotropy for the blue phases. In our first article we found a small elastic anisotropy $\lambda_K/\lambda \approx \pm 0.3$. Hence the viscous behavior must be highly anisotropic. The relaxation frequency of the third mode tends to zero with $\boldsymbol{q}$. It corresponds to the low frequency noise also measured by Marcus [3].

The dynamics of the light-scattering experiments of Marcus [3] and Domberger [4] can be well understood by the dynamics of the displacement modes. So far only estimates for the introduced material parameters are available. Further experiments are necessary to measure them, especially the permeation coefficient, and to verify our conclusion that the cubic blue phases are highly anisotropic with regard to their viscous properties. The dynamical theory of light scattering gives a very complex behavior of the light scattering intensities, which also needs to be confirmed.

ACKNOWLEDGMENTS

We thank Wolfgang Domberger for helpful discussions about his light-scattering experiments. This work has been supported by the Deutsche Forschungsgemeinschaft under Project No. Tr 154/9-1.

[1] H. Stark and H.-R. Trebin, preceding paper, Phys. Rev. E **51**, 2316 (1995).
[2] M. A. Marcus, Phys. Rev. A **84**, 1109 (1984).
[3] M. A. Marcus, Mol. Cryst. Liq. Cryst. **122**, 131 (1985).
[4] W. Domberger, Ph.D. thesis, Westfälische Wilhelms-Universität, Münster, 1991.
[5] A. C. Eringen and C. B. Kafadar, in *Continuum Physics: Volume IV — Polar and Nonlocal Field Theories*, edited by A. C. Eringen (Academic, New York, 1976).
[6] H. Ehrentraut, diploma thesis, Technische Universität Berlin, 1989.
[7] U. Semmler, diploma thesis, Universität Regensburg, 1981.
[8] I. Müller, *Thermodynamik: Grundlagen der Materialtheorie* (Bertelsmann Universitätsverlag, Düsseldorf, 1973).
[9] R. M. Bowen, in *Continuum Physics: Volume III — Mixtures and EM Field Theories*, edited by A. C. Eringen (Academic, New York, 1976).
[10] H. Stark and H.-R. Trebin (unpublished).
[11] H. Stark, Ph.D. thesis, Universität Stuttgart, 1994.
[12] W. Helfrich, Phys. Rev. Lett. **23**, 372 (1969).
[13] M. J. Stephen and J. P. Straley, Rev. Mod. Phys. **46**, 617 (1974).
[14] D. Demus, H.-G. Hahn, and F. Kuschel, Mol. Cryst. Liq.

Cryst. **44**, 61 (1978).
[15] H. Stegemeyer and P. Pollmann, Mol. Cryst. Liq. Cryst. Lett. **82**, 123 (1982).
[16] T. Ohtsuki, S. Mitaku, and K. Okano, Jpn. J. Appl. Phys. **17**, 627 (1978).
[17] J. F. Joanny, J. Colloid Interface Sci. **71**, 622 (1979).
[18] E. Dubois-Violette, P. Pieranski, F. Rothen, and L. Strzelecki, J. Phys.(Paris) **41**, 369 (1980).
[19] H. M. Lindsay and P. M. Chaikin, J. Chem. Phys. **76**, 3774 (1982).
[20] M. Jorand, E. Dubois-Violette, B. Pansu, and F. Rothen, J. Phys. (Paris) **49**, 1119 (1988).
[21] N. A. Clark, S. T. Vohra, and M. A. Handschy, Phys. Rev. Lett. **52**, 57 (1984).
[22] P. E. Cladis, P. Pieranski, and M. Joanicot, Phys. Rev. Lett. **52**, 542 (1984).
[23] R. N. Kleiman, D. J. Bishop, R. Pindak, and P. Taborek, Phys. Rev. Lett. **53**, 2137 (1984).
[24] I. N. Bronstein and K. A. Semendjajew, *Taschenbuch der Mathematik* (Verlag Harri Deutsch, Frankfurt am Main, 1984).
[25] B. J. Berne and R. Pecora, *Dynamic Light Scattering — With Applications to Chemistry, Biology, and Physics* (Wiley, New York, 1976).
[26] A. Münster, *Statistical Thermodynamics*, 1st English ed. (Springer-Verlag, Berlin, 1969), Vol. I.
[27] L. D. Landau and E. M. Lifschitz, *Statistische Physik: Teil 1*, Vol. 5 of *Lehrbuch der Theoretischen Physik* (Akademie-Verlag, Berlin, 1987).
[28] R. Barbet-Massin and P. Pieranski, J. Phys. (Paris) Colloq. **46**, C3-61 (1985).
[29] H. Zink and W. van Dael, Liq. Cryst. **14**, 603 (1993).
[30] E. Fick, *Einführung in die Grundlagen der Quantentheorie* (Akademische Verlagsgesellschaft, Frankfurt am Main, 1974).
[31] J. D. Jackson, *Classical Electrodynamics*, 2nd ed. (Wiley, New York, 1975).
[32] H.-R. Trebin, W. Fink, and H. Stark, Int. J. Mod. Phys. B **7**, 1475 (1993).
[33] R. M. Hornreich and S. Shtrikman, Phys. Rev. A **28**, 1791 (1983).
[34] M. v. Laue, Ergeb. Exakten Naturwiss. **10**, 133 (1931).
[35] W. H. Zachariasen, *Theory of X-Ray Diffraction in Crystals* (Dover, New York, 1967).
[36] J. F. Cornwell, *Group Theory in Physics: Volume I* (Academic, London, 1984).
[37] E. Fues, Z. Phys. **109**, 14 (1938).